Available online at www.sciencedirect.com
ScienceDirect
Journal of Power Sources 160 (2006) 1447–1450
JOURNAL OF POWER SOURCES
www.elsevier.com/locate/jpowsour

Short communication

Novel electrolyte for zinc–polyaniline batteries

B.Z. Jugović [a], T.Lj. Trišović [a], J. Stevanović [b], M. Maksimović [c], B.N. Grgur [c,*]

[a] *Institute of Technical Science, Serbian Academy of Science and Arts, Knez Mihailova 35, 11000 Belgrade, Serbia and Montenegro*
[b] *Institute of Electrochemistry, ICTM, Njegoševa 12, 11000 Belgrade, Serbia and Montenegro*
[c] *Faculty of Technology and Metallurgy, Karnegijeva 4, 11000 Belgrade, Serbia and Montenegro*

Received 14 December 2005; accepted 22 February 2006
Available online 18 April 2006

Abstract

Electrochemical behavior of zinc and polyaniline (PANI) electrode polymerized from 0.1 M HCl and 0.1 M aniline on graphite electrode, in 0.2 M $ZnCl_2$ and 0.50 M NH_4Cl (chloride electrolyte) and with addition of 0.33 M Na-citrate (chloride/citrate electrolyte) were investigated. In the chloride/citrate comparing with chloride containing electrolyte for the zinc electrode negative shift of the open circuit potential of 150 mV, decreases of exchange current density for more than order of magnitude and increase of cathodic Tafel slope, due to the zinc ions complexation, were observed. In citrate/chloride electrolyte zinc dendrite formation were completely suppressed. PANI electrodes show better discharge characteristic in chloride/citrate electrolyte with determined maximum discharge capacity of 164 mAh g^{-1}.

Keywords: Polyaniline; Zinc; Batteries; Chloride; Citrates; Dendrites

1. Introduction

Zinc–polyaniline (PANI) secondary cells has a lot of advantages, in comparison with classical battery types (Cd|NiOOH, Pb|PbO_2, Zn|Ag_2O, MH|NiOOH) and aprotonic cells (Li|C and Li|polymer). First advantage is ecological acceptability comparing with Cd|NiOOH or Pb|PbO_2, second is relatively low price (Zn|Ag_2O and MH|NiOOH), and third is uses of water based electrolytes (mainly ammonium chloride + zinc chloride) [1], that makes such cells much easier to manufacture than Li based one.

Up to now zinc–PANI batteries has not been commercialized from few main reasons. First reason is degradation process of PANI at potentials more positive than ~0.5 V [2,3], and second is zinc passivation, which is possibly related to the formation of the solid phases $ZnCl_2 \cdot 3NH_4Cl$ and $ZnCl_2 \cdot 2NH_4Cl$ on the anode surface [4]. On the other hand, in chloride containing electrolytes Zn electrodes form dendrites during charge–discharge cycles [5,6]. It results in decreased coulombic efficiency of batteries and charge life. Main reason for that are sort circuit provoked by penetration of dendrites through separator to cathode or formation of the anodic slime.

It is well known that some organic anions can form complexes with the metal ions, that results much better quality of the metal deposits and suppress dendrite formation [7]. Probably, the best choice will be oxalic anions, due to the small ionic radius, good PANI doping–dedoping characteristics, etc. [8]. Unfortunately, zinc oxalate is an insoluble salt.

So, in this paper we investigated behavior of zinc and PANI electrodes in chloride containing electrolytes with addition of citrate anions, which at pH ~ 5 form an soluble zinc citrate $[ZnCit]^-$ complex with pK_s value of 4.8.

2. Experimental

Polyaniline was obtained from hydrochloric acid solution (0.1 M) with addition of 0.1 M aniline monomer (p.a. Merck, distilled in argon atmosphere), at constant current density of 1 mA cm^{-2} on graphite electrode. Electrolytes containing 0.5 M NH_4Cl, 0.20 M $ZnCl_2$ and with addition of 0.33 M Na-citrate were prepared from p.a. grade chemicals (Merck) and bidistilled water. For all experiments three compartment electrochemical cell, with platinum foil ($S = 2\ cm^2$) as a counter and saturated

* Corresponding author. Tel.: +381 113303681; fax: +381 113370387.
E-mail address: BNGrgur@tmf.bg.ac.yu (B.N. Grgur).

0378-7753/$ – see front matter © 2006 Elsevier B.V. All rights reserved.
doi:10.1016/j.jpowsour.2006.02.096

calomel electrode as a reference electrode at room temperature was used.

The working electrodes, graphite ($S = 0.64\,cm^2$) and zinc ($S = 2\,cm^2$), were mechanically polished with fine emery papers (2/0, 3/0 and 4/0, respectively) and then with polishing alumina of 1 μm (Banner Scientific Ltd.) on the polishing cloths (Buehler Ltd.). After mechanical polishing the traces of polishing alumina were removed from the electrode surface in an ultra-sonic bath during 5 min. The electrochemical measurements were carried using a PAR 273A potentiostat controlled by a computer through a GPBI PC2A interface.

3. Results and discussion

In Fig. 1 comparison of zinc deposition–dissolution on graphite electrode from chloride and chloride/citrate containing electrolytes are shown. As it can be seen from chloride electrolyte, deposition processes starts at potentials around −1 V, thought one well-defined peak, at −1.17 V, after at potentials more negative than −1.4 V proceed simultaneous zinc deposition and hydrogen evolution reactions. In anodic direction, zinc dissolution occurs at potentials more positive than −1 V through one pack and one shoulder. In citrate/chloride electrolyte deposition–dissolution reaction is shifted for ∼0.15 V in negative direction and diffusion limited peak is two times smaller, than in chloride electrolytes. This behavior could be explained by zinc ions complexation and lowering of the free zinc ions activity, as well as diffusivity of zinc citrate complex comparing with chloride electrolyte.

Slow potentiodynamic ($v = 1\,mV\,s^{-1}$) polarization curves in chloride and chloride/citrate electrolyte on solid zinc electrode are shown in Fig. 2. Open circuit potential, E_{ocp}, for zinc electrode in chloride electrolyte where −0.997 V which was ∼130 mV more positive than in chloride/citrate electrolyte, $E_{ocp} = -1.130$ V. Determined Tafel slopes for the chloride electrolyte were $\pm 35\,mV\,dec^{-1}$, and exchange current density,

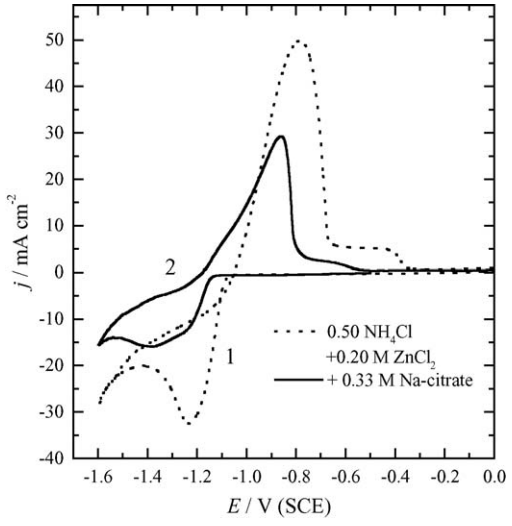

Fig. 1. Cyclic voltammograms of graphite electrode in (1) 0.50 M NH_4Cl + 0.20 M $ZnCl_2$ and (2) with addition of 0.33 M Na-citrate. Sweep rate $20\,mV\,s^{-1}$.

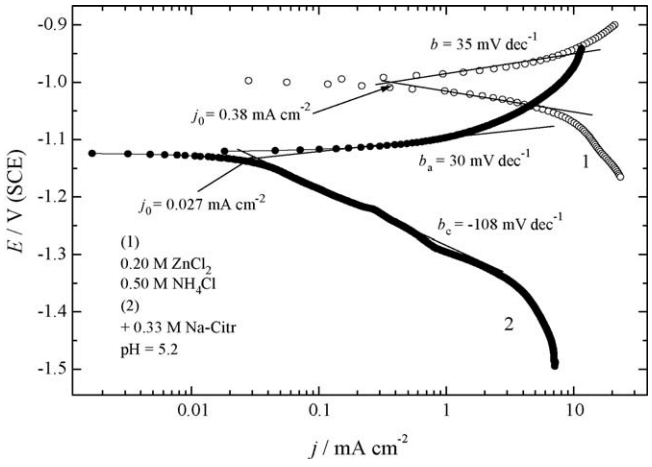

Fig. 2. Slow potentionamic polarization curve ($v = 1\,mV\,s^{-1}$) in chloride (1) and chloride/citrate (2) containing solution on solid zinc electrode.

extrapolated from intercept of Tafel lines with open circuit potentials, was 0.38 mA cm^{-2}. In the chloride/citrate electrolyte anodic Tafel slope was ∼30 mV dec^{-1}, and cathodic Tafel slope −108 mV dec^{-1}. Exchange current density of 0.027 mA cm^{-2}, was more than one order of magnitude smaller than in chloride electrolyte.

In Fig. 3 micrographs of zinc deposits obtained from chloride and chloride/citrate electrolytes at a constant current density of 3.5 mA cm^{-2} and with deposition charges of 10.5 mAh cm^{-2} are shown.

Deposition current density 3.5 mA cm^{-2}, deposition time 3 h, magnification 200×.

In chloride electrolyte, Fig. 3a, obtained deposits are practically completely dendritic, so potential risk of fast dendrite growth through separator, during the longer charging times, and formation of short circuits with cathode is permanently present. On the other hand in chloride/citrate electrolyte, Fig. 3b, deposit is smooth without irregularities even in the edges where local current density due to the current distribution phenomena is higher than at the central surface. Such differences can be explained in the following way.

The classical expression for the steady state nucleation rate, J, is given by [7]:

$$J = K_1 \exp\left(\frac{K_2}{\eta^2}\right) \quad (1)$$

where K_1 and K_2 are overpotential, η, ($\eta = E - E_{ocp}$) independent constants. Eq. (1) is valid for a number of systems regardless of the value of the exchange current density for the deposition process. At one and the same deposition current density, j, decreasing j_0 leads to an increasing nucleation rate and decreasing nucleation exclusion zones radii [7]. The saturation nucleus density, i.e., the exchange current density of the deposition process, strongly affects the morphology of metal deposits. At high exchange current densities, the radii of the screening zones are large and the saturation nucleus density is low. This permits the formation of large, well-defined crystal grains and granular (dendrite) growth of the deposit. At low exchange current densities, the screening zones radii are low, or equal to zero, the

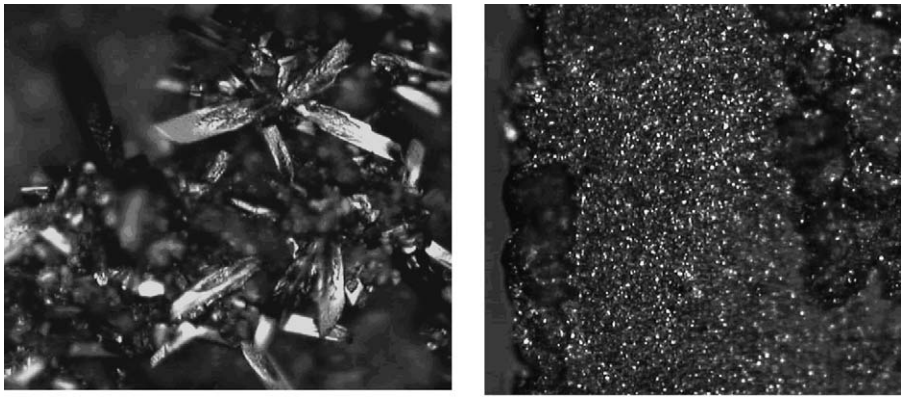

Fig. 3. Micrographs of the zinc deposits from (a) 0.20 M $ZnCl_2$ + 0.50 M NH_4Cl and (b) with addition of 0.33 M Na-citrate.

nucleation rate is large and a smooth surface film can be easily formed.

The overpotential and the current density in activation-controlled deposition inside the Tafel region are related by

$$\eta = \frac{b_c}{2.3} \ln \frac{j}{j_0} \quad (2)$$

Therefore, increasing b_c and decreasing j_0 leads to an increase in the deposition overpotential at the constant current density. It follows from all available data that the former effect is more pronounced resulting in deposits with a finer grain size with decreasing value of the exchange current density.

This analysis explain differences in deposit morphology for chloride and chloride/citrate electrolytes taking into account that Tafel slopes are −35 and −108 mV dec^{-1}, and exchange current densities are 0.38 and 0.027 mA cm^{-2}, respectively. Hence, in chloride electrolyte at 3.5 mA cm^{-2} deposition overpotential is only −30 V, while in chloride/citrate electrolyte is −220 mV.

Inset of Fig. 4 shows the galvanostatic curve for polymerization of aniline from solution containing 0.10 M HCl and 0.10 M aniline monomer on graphite electrode at current density of 1 mA cm^{-2} with polymerization charge of 0.3 mAh cm^{-2}. Polymerization starts at potential of 0.75 V and proceed in the potential range between 0.75 and 0.7 V. After polymerization, electrode was washed with bidistilled water and transferred in the three compartment electrochemical cell with chloride or chloride/citrate electrolyte. After transfer, electrode was conditioned at potential of −0.8 V for 600 s and cyclic voltammograms in the potential range between −0.8 and 0.4 V were taken as shown in Fig. 4. In anodic direction doping of the anions occur at potentials more positive than −0.2 V, with pronounced peak at 0.15 V. In cathodic direction dedoping of anions occur through one shoulder in the potential range of 0.4–0.05 V and one well-defined peak with the maximum at −0.1 V. Dedoping of anions is finished at potentials of −0.4 V. Small differences in the shapes of cyclic voltammograms between chloride and chloride/citrate electrolytes, could indicate that only chloride anions are involved in doping/dedoping reaction.

Fig. 5 shows charge–discharge curves in chloride and chloride/citrate electrolytes at current density of 0.25 mA cm^{-2}. Charging curves in both solutions are practically identical, but

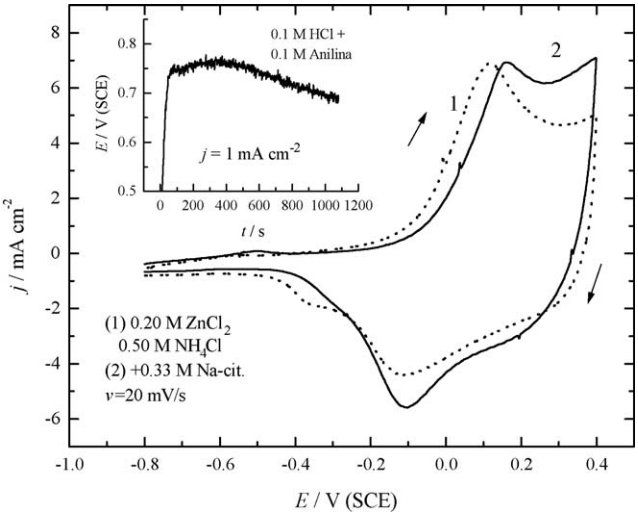

Fig. 4. Cyclic voltammograms of PANI electrode in (1) chloride and (2) chloride/citrate electrolyte ($v = 20$ mV s^{-1}). Inset: galvanostatic curve for aniline polymerization from 0.1 M HCl and 0.1 M aniline at 1 mA cm^{-2} on graphite electrode.

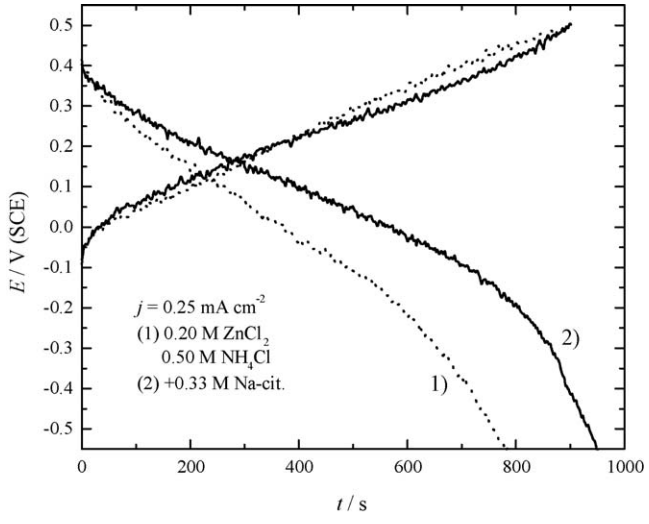

Fig. 5. Charge–discharge curve for (1) chloride and (2) chloride/citrate electrolyte at current density of 0.25 mA cm^{-2}.

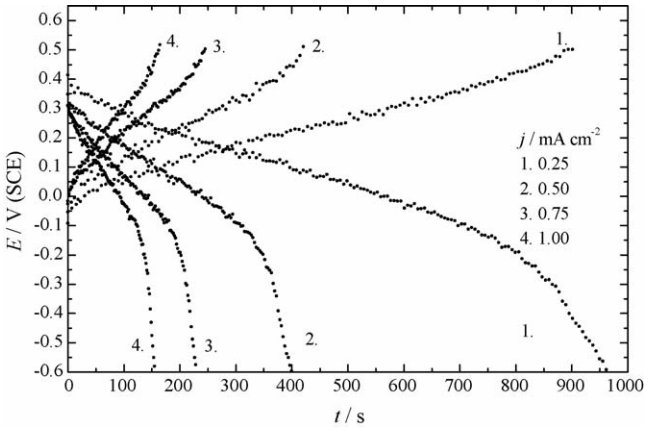

Fig. 6. Dependencies of the potential for different charge/discharge current density for PANI electrode.

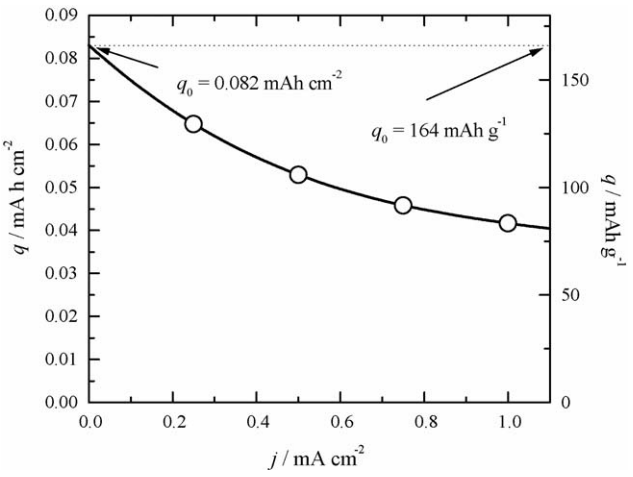

Fig. 7. Dependence of charge (left) and specific charge (right) at different discharge current density for PANI electrode in chloride/citrate electrolyte.

discharging curve in chloride/citrate solution have higher discharge potentials and longer discharge time. Up to now we do not have explanation for that kind of behavior.

Dependences of the potential for different charge/discharge current density for PANI electrode in chloride/citrate electrolyte are shown in Fig. 6. Charging/discharging reaction, assuming that only chloride anions are involved, can be given with following scheme [9]:

$$\mathrm{PANI} + n\mathrm{Cl} \underset{\text{discharge}}{\overset{\text{charge}}{\rightleftarrows}} \mathrm{PANI(Cl)}_n + ne \quad (3)$$

Charging reaction occur in the potential range between 0 and 0.5 V (upper potential limit is taken to avoid degradation of PANI film) with constant increase of the potential. Discharge of the electrode occurs in the potential region between 0.35 and ~−0.2 V with average discharge potential of ~0.15 V. After potentials more negative than −0.2 V diffusion limitations provoke the sharp decrease of the potential. Tacking into account that average discharge potential for zinc electrode is ~−1.1 V, it can be calculated that average discharge voltage for the zinc–PANI cell with chloride/citrate electrolyte will be 1.25 V. This value is higher than open circuit potentials for Cd|NiOOH or MH|NiOOH cells, and comparable with alkaline Zn|MnO_2 cell.

Charging/discharging characteristics of PANI film electrode are affected with applied current density, mainly because chloride anions diffusion limitation through PANI film. In Fig. 7 dependence of capacity during discharge processes for different discharging current densities are shown.

Discharge capacity increase with decreasing applied current density and for the limiting case when $j_d \to 0$, discharge capacity has a value of 0.082 mAh cm^{-2}.

Assuming the 100% current efficiency during the polymerization of aniline and using the equations [10,11]:

$$m = \frac{jt(M_m + yM_a)}{(2+y)F} \quad (4)$$

where m is the mass of the polyaniline polymerized with current density j during the time, t, M_m and M_a are molar mass of aniline monomer and inserted, chlorine, anions, and $y = 0.5$ is doping degree for emeraldine salt, it could be calculated that mass of the PANI on graphite electrode was approximately 0.5 mg. Hence, for the limiting case with discharge capacity of 0.082 mAh cm^{-2} specific discharge capacity could be estimate on 165 mAh g^{-1}. In the range of investigated current densities of 0.25–1 mA cm^{-2}, specific discharge capacity was in the range of 130–85 mAh g^{-1}, respectively.

Acknowledgment

This work is financially supported by the Ministry of Science and Environmental protection, Republic of Serbia, contract No. 142044.

References

[1] M. Sima, T. Visan, M. Buda, J. Power Sources 56 (1995) 133.
[2] L.D. Arsov, W. Plieth, G. Kossmehl, J. Solid State Electrochem. 6 (1998) 355.
[3] H.N. Dinh, J. Ding, S.J. Xia, V.I. Birss, J. Electroanal. Chem. 459 (1998) 45.
[4] M.S. Rahmanifar, M.F. Mousavi, M. Shamsipur, M. Ghaemia, J. Power Sources 132 (2004) 296.
[5] J. Kan, H. Xue, S. Mu, J. Power Sources 74 (1998) 113.
[6] G. Mengoli, M.M. Musiani, D. Pletcher, S. Valcher, J. Appl. Electrochem. 17 (1987) 515.
[7] K.I. Popov, S.S. Djokić, B.N. Grgur, Fundamental Aspects of Electrometallurgy, Kluwer Academic/Plenum Publishers, New York, 2002.
[8] E. Erdem, M. Saçak, M. Karakişla, Polym. Int. 39 (1996) 153.
[9] A. Mirmohseni, R. Solhjo, Eur. Polym. J. 39 (2003) 219.
[10] J. Kankare, in: D. Wise, G.E. Wnek, D.J. Trantolo, T.M. Cooper, J.D. Gresser (Eds.), Electrical and Optical Polymer Systems: Fundamentals, Methods, and Applications, Marcel Dekker, New York, 1998 (Chapter 6).
[11] M.M. Popović, B.N. Grgur, Synth. Met. 143 (2004) 191.